UNSTEADY DISSIPATION MEASUREMENTS ON A FLAT PLATE SUBJECT TO WAKE PASSING

R. D. Stieger
Whittle Laboratory, University of Cambridge, Cambridge, England
rds28@eng.cam.ac.uk
H.P. Hodson
Whittle Laboratory, University of Cambridge, Cambridge, England
hph@eng.cam.ac.uk

ABSTRACT

Boundary layer measurements were performed on a flat plate with an imposed pressure gradient typical of a high lift low pressure (LP) turbine blade and subject to incoming turbulent wakes shed from a moving bar wake generator. A multiple-orientation 1D LDA technique was used to measure the ensemble average mean flow and Reynolds stresses. These ensemble average measurements were used to calculate the boundary layer dissipation thereby providing unprecedented experimental evidence of the loss reducing mechanisms associated with wake induced transition. The benign character of the calmed zone was confirmed and the early stages of boundary layer separation were found to have laminar levels of dissipation. A deterministic natural transition phenomenon was identified between wake passing events highlighting the existence of natural transition phenomena in LP turbine style pressure distributions.

INTRODUCTION

The primary concern for aero-engine operators is the total cost of engine ownership, which includes not only the capital cost but also the operating costs that are influenced, amongst others, by efficiency and weight. Based on the extensive experimental work of Curtis et al [1] and Howell et al [2] 'high lift' LP turbine blade profiles were developed out of an improved understanding of unsteady transition phenomena. These profiles were reported to reduce the blade count of the LP turbine by 20% (Cobley et al,[3]) thus achieving the ultimate goal of reducing the cost of ownership by simultaneously reducing weight and manufacturing costs while providing little efficiency penalty.

Schulte and Hodson [4] showed that the periodic passing of wakes affected the separation bubble on a high lift LP turbine blade and reported a reduction in profile loss due to the wake passing for some flow conditions. This phenomenon was later explained with hot film measurements showing that turbulent spots induced by the wake upstream of the separation point prevented the boundary layer from separating and that the calmed regions that follow the turbulent spots were able to withstand more severe pressure gradients without separation. It is therefore possible to design LP turbine blades with more aggressive suction surface decelerations than had previously been thought possible without increased loss due to large separation bubbles.

The loss reductions are intimately linked to the relative portions of the blade surface covered by laminar, turbulent, calmed and separated flow. The measurements presented here provide experimental proof of these loss-reducing mechanisms that are exploited in the design

of high lift LP turbine blades. Moreover, the transition path between wake passing events is shown to be by means of natural transition phenomena involving the unsteady development of Tollmien-Schlichting waves, which are phase locked and apparent in the ensemble average measurements.

EXPERIMENTAL FACILITY

The test facility consisted of a flat plate, shown in Figure 1 that was attached to the exit of an open return wind tunnel downstream of a moving bar wake generator. The flat plate had a chord (c) of 548mm and the span was 458mm. The plate was 30mm thick with a 14:3 ellipse at the leading edge. The trailing edge was blunt and a splitter plate, 100mm in length, was attached to the centre of the trailing edge to suppress vortex shedding. A pair of contoured walls imposed a pressure distribution on the flat plate. The symmetrical arrangement was chosen to ensure zero incidence at the leading edge. The shape of the contoured walls was designed using a simple one-dimensional continuity argument to match the pressure distribution measured on the T106 LP turbine cascade.

A moving bar wake generator was used to create unsteady wake passing conditions. Carbon fibre bars of 7.8mm diameter were used and passed 245mm in front of the plate leading edge. The bar diameter was chosen so that the wake centre line turbulence level at the leading edge of the flat plate was Tu=5% and thus representative of the inlet turbulence intensity of the cascade measurements of Curtis et al [1]. The Reynolds number based on surface length and exit velocity was Re=214000, the flow coefficient (ϕ) based on exit velocity (V_2) and bar speed (U_b) was $\phi=V_2/U_b=0.83$ and the reduced frequency (f_r) was $f_r=fc/V_2=0.67$ where (f) is the frequency in Hz.

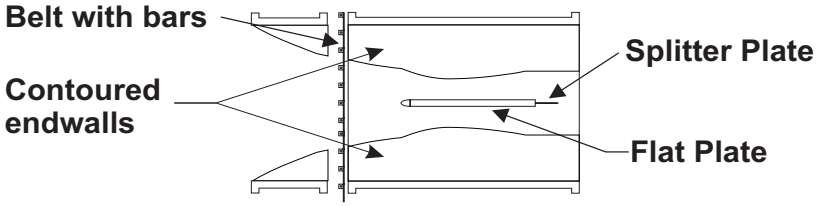

Figure 1: Sketch of Flat Plate with symmetrical end walls used to impose an LP turbine style pressure distribution.

LDA Measurements

Measurements of the flat plate boundary layer were made using a single component Dantec LDA system with a 5W Argon-Ion laser. A 2D 85mm Dantec probe was used with a 1.95 beam expender and a focal length of 500mm giving a measuring volume 0.077mm by 1.016mm for the 514.5nm beam. A backward scatter configuration was used and a Dantec BSA 57N21 signal processor processed the Dantec 9057X0081 photo-multiplier output.

Seeding of the flow was by means of smoke generated using Shell Ondina oil to produce a characteristic particle size of approximately 1.5μm. The smoke entered the flow through the trailing edge of a streamlined injector tube at a point approximately 3m upstream of the test section. The ensemble average mean velocity vector and 2D Reynolds stresses were measured using the rotated 1D LDA technique detailed by Stieger and Hodson [5]. This technique uses measurements of velocity variance ($\overline{m_i'^2}$) made at more than three orientations of the measurement volume. The volume is rotated about its longitudinal axis. A least squares fit is then used to provide the three components of the Reynolds stress tensor ($\overline{u'^2}$, $\overline{v'^2}$ & $\overline{u'v'}$) since

$$\overline{m_i'^2} = \overline{u'^2}\cos^2(\overline{\theta}_i) + \overline{v'^2}\sin^2(\overline{\theta}_i) - 2\overline{u'v'}\sin(\overline{\theta}_i)\cos(\overline{\theta}_i) \quad (1)$$

where, $\overline{\theta}_i$, denotes the angle between the plane of the laser beams and the mean velocity vector.

At each traverse position 7 probe orientations were used ranging from +45° to -45° with a maximum of 100000 samples collected at each orientation. For this quantity of collected data, the results of Stieger and Hodson [5] indicate that the average variance of the rotated 1D LDA measurements from equivalent 2D LDA measurements is approximately 2×10^{-4}. The boundary layer was traversed at 13 locations evenly distributed along the blade surface between 50 and 94 % surface length. Each traverse consisted of 25 points exponentially distributed normal to the wall with the first point 0.1 mm and the final point 25.0 mm above the surface of the plate. A maximum of 60 seconds of data was acquired at each traverse point. This corresponded to a maximum of approximately 2500 wake passing cycles. The data rate typically varied from 1.5 to 5Khz.

DISCUSSION OF RESULTS

Wake Induced Transition and Calming

The surface pressure distribution measured on the flat plate is shown in Figure 2 with and without wake passing. The steady inflow condition shows a separation bubble extending from a surface fraction of s/s_0=0.61 to s/s_0=0.82. However, with the bar passing the separation bubble is suppressed in the time mean and the pressure distribution is in good agreement with that of the T106 cascade with wake passing, particularly downstream of peak suction which is the area of interest.

The boundary layer shape factor (H_{12}) gives a clear characterisation of the boundary layer profile and serves to indicate the boundary layer state. In order to identify the ensemble average boundary layer state in space and time an s-t diagram of H_{12} is plotted in Figure 3 where the data is duplicated onto two periods to assist interpretation. Lines A and B are drawn to mark the trajectory of the wake in the freestream while line D is drawn at the celerity of the trailing edge of turbulent spots. The celerity of line D was calculated from the measured time average boundary layer integral parameters and the correlation of Gostelow et al [6]. Line E marks the trailing edge of the calmed region and its celerity was calculated by assuming a constant ratio between the celerity of the trailing edge of a turbulent spot and the trailing edge of the calmed region. The trajectory lines were then calculated from the time averaged boundary layer edge velocity and the respective celerities.

The region of low H_{12} bounded by lines B and D is a classical wake induced turbulent wedge. The high levels of turbulence in the wake intermittently induce turbulent spots in the attached boundary layer upstream of the separation point by means of a bypass transition mechanism. Due to the adverse pressure gradient the spots grow rapidly in the spanwise direction and coalesce into a spanwise turbulent strip. This is indicated by low H_{12} measured under the wake as far upstream as the first measurement location. The leading edge of the turbulent strip travels faster than the trailing edge, thus as the turbulent strip convects downstream its streamwise extent increases. This results in a characteristic wedge shape on an s-t diagram. The elevated turbulence and full boundary layer profiles of the turbulent strip convect into the separated region and suppress the separation bubble that has been developing since the previous wake-passing event.

The region between the wake passing events in Figure 3 shows the relaxation of the turbulent boundary layer under an adverse pressure gradient. The calmed region dominates

this process. The calmed region may be described as the unsteady response of the boundary layer to the removal of turbulent stresses. Immediately after the wake induced turbulent strip has passed, the boundary layer profile is full with a low shape factor. The removal of turbulent shear (turbulent viscosity) allows the profile to relax back to the laminar like profile with high shape factor. The final state of the boundary layer is determined by the local pressure gradient. In Figure 3, this effect is apparent in the region bounded by lines D and E. Upstream of s/s_0=0.65, the calmed region has a short duration and the boundary layer quickly returns to the high shape factor state. However, by s/s_0=0.70, the calmed region lasts longer and the local pressure gradient is stronger. The boundary layer thus becomes inflexional and begins to separate towards the end of the calmed region. Indeed, the downstream edge of the high H_{12} region is seen to coincide with line E. This indicates that the fuller profiles of the calmed region resist separation and thus control the separating boundary layer.

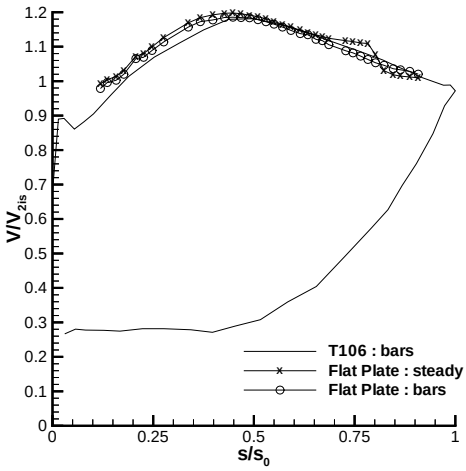

Figure 2: Isentropic velocity distribution measured on the flat plate with steady inflow and wake passing.

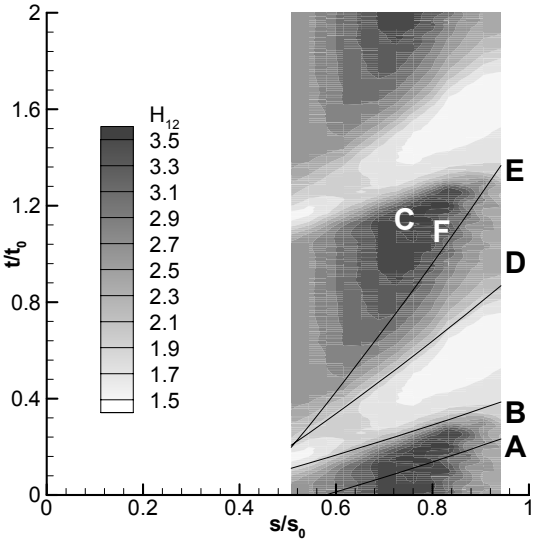

Figure 3: s-t diagram of measured boundary layer shape factor

Between lines A and B in Figure 3, the interaction of the negative jet and the separating boundary layer is evident. In the region s/s_0=0.65 to s/s_0=70, the shape factor is seen to increase beneath the centre of the wake (midway between lines A and B). This is the result of the outer region of the boundary layer responding to the wake more rapidly than the near the wall region where viscous effects dominate. This distortion of the boundary layer results in an increase in H_{12}.

The observed unsteady transition process is thus classical and is characterised by a wake-induced transition upstream of the boundary layer separation point. The wake induced turbulent strip then convects into the region of the separation and suppresses the separation bubble, which does not re-establish until the passing of the calming effects.

Deterministic Natural Transition Phenomena

During the wake passing cycle the boundary layers are alternately subjected to turbulent wake flow and relatively undisturbed flow from the upstream blade row. Thus, although rapid bypass transition may be induced under the wake passage, the portion of the cycle between wake passing events may result in a transition process more akin to natural boundary layer transition. The investigation of Hughes and Walker [7] presents evidence of such natural transition phenomena in hot-film signals measured on a 1.5 stage axial compressor. A wavelet

analysis of hot-film signals revealed significant regions where the frequency content was within ±10% of that predicted for Tollmien-Schlichting (T-S) waves. The T-S waves were identified over a wide range of operating conditions, even when turbulence levels were as high as 8%.

A close inspection of Figure 3 in the region labelled F shows that the ensemble averaged H_{12} displays regular temporal oscillations between wake passing events. The oscillations arise along a line parallel to line E and the onset of the oscillations therefore appears to be associated with the ending of the calmed region.

The development of the velocity fluctuations in time and space can be seen in Figure 4(a), where the ensemble average time traces of the first five traverse points from the wall (0.1mm to 0.6mm) are plotted at each of the streamwise measurement locations along the surface of the flat plate. At all surface locations the velocity fluctuations emerge after the calmed region has passed. The disturbance amplitude grows with surface distance but the frequency is observed to be approximately constant at all surface locations. From the period of the velocity fluctuations, the frequency was found to be approximately 80Hz.

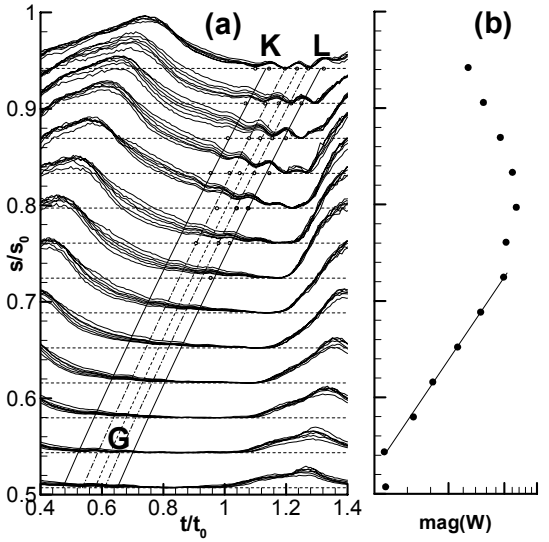

Figure 4: (a) The development of near wall velocity fluctuations ($0.1s/s_0=0.5\%V_{2is}$) and (b) the exponential growth of oscillations in the T-S frequency range.

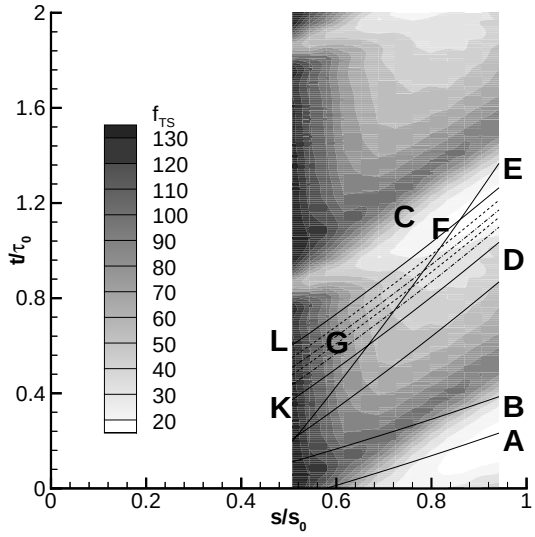

Figure 5: s-t diagram showing the frequency of the most amplified T-S waves from Walker's correlation.

The trajectory of the wave packets is marked in Figure 4(a) by the peaks and troughs in the velocity traces. At the time of each peak and trough, a circle is drawn at the appropriate surface distance. Also drawn in Figure 4(a) are trajectory lines K and L which have a trajectory of 0.5U. The circles designating peaks and troughs lie very nearly on these trajectory lines. Solutions of the Orr-Sommerfeld equations for the Falkner-Skan profile on the verge of separating (β=–0.1988) show that this is in good agreement with the calculated phase speed of the most amplified wave (see Obremski et al [9]).

The growth of the oscillations in the region between lines K and L in Figure 4(a) was measured using a Morlet wavelet (ω_0=6.0) transform of the ensemble average velocity traces 0.5mm above the surface of the plate. By integrating the magnitude of the wavelet coefficients in the range 80% to 120% of the observed frequency of 80Hz over the time between lines K and L, the energy in the disturbance was measured. Figure 4(b) plots the energy against surface length on log-linear scale. The straight line fitted in the region s/s_0=0.55 to s/s_0=0.72 demonstrates that in this region the growth of the waves is exponential.

The above experimental observations are characteristic of the growth and propagation of instability wave packets that occur in natural boundary layer transition. Experimental investigations have shown that the dominant disturbance frequency at breakdown is well predicted by the T-S wave frequency having the maximum amplification ratio (Walker [8]). The frequency of the T-S waves may be predicted by linear stability theory. However, this involves a search for eigenvalues of the Orr-Sommerfeld equation. It has been observed that the stability characteristics of a boundary layer are most strongly influenced by the shape of the velocity profile (Obremski et al [9]). For the purposes of approximating the stability characteristics, the velocity profiles measured on the flat plate may be approximated by the Falkner-Skan boundary layer profiles. A stability analysis on such profiles was performed by Obremski et al [9]. Based on these calculations, Walker [8] derived a correlation for the frequency (f) of the most amplified T-S waves in terms of the displacement thickness Reynolds number (Re_{δ^*}), boundary layer edge velocity (U_{98}) and viscosity (υ) according to

$$f = \frac{3.2 {U_{98}}^2 \mathrm{Re}_{\delta^*}^{-3/2}}{2\pi\upsilon} \tag{2}$$

From the above correlation and the ensemble average displacement thickness measured on the flat plate, it is possible to calculate the distribution of the most amplified T-S wave frequencies. Figure 5 shows the results of this calculation. The trajectories drawn on Figure 3 are copied to Figure 5. The observed frequency of about 80Hz is seen to correspond to the region labelled G. From the trajectory lines, it is apparent that the waves observed are T-S waves that originate in the region of G and convect downstream while being amplified by the viscous instability mechanisms associated with the boundary layer.

The agreement between the predicted frequency and that of the ensemble-average measurements indicates that the transition mechanism occurring between wake passing events in a highly decelerated boundary layer is characteristic of a deterministic natural boundary layer transition. In this respect, the results are similar to those of Obremski and Morkovin [10] who observed well-defined wave-packets prior to transition on a flat plate subject to a sinusoidally oscillating freestream. They concluded that the repeatability of the measured wave packets was due to the unsteady flow. At a particular point in the unsteady cycle, the boundary layer is most susceptible to disturbances. Therefore, disturbances arising at this point in the cycle are amplified by the boundary layer and so the unsteady flow acts to filter the initial disturbances. This same mechanism is present in the unsteady flow that results from wake-induced transition. The boundary layer velocity profile changes cyclically from the full turbulent profile, through the calmed profiles and tends towards the separated profiles that would exist in steady flow. Disturbances will thus amplify at the first phase when the velocity profile becomes unstable and the disturbance spectrum continues to amplify according to the local linear stability characteristics of the boundary layer. Obremski and Morkovin [10] achieved reasonable success in predicting the frequency and amplification ratio of the observed wave packets developing on their flat plate subject to an oscillating freestream by using a quasi-steady adaptation of the e^n method. Traditional steady flow values of n in the e^n method were found to be inadequate for describing the transition onset location. However, as in all current transition prediction methods this could be overcome by appropriate experimental correlations. The evidence of deterministic instability waves presented above suggests that a quasi-steady e^n method such as that of Obremski and Morkovin could be used to describing the transition between wake passing in turbomachinery environments.

Boundary Layer Dissipation Measurements

The ultimate measure for loss of efficiency in turbomachinery is the creation of entropy (Denton [11]). Viscous dissipation in the blade surface boundary layers is the primary source of entropy generation in LP turbines. It is possible to determine the non-dimensional viscous dissipation per surface area, C_D, in a boundary layer by evaluating the integral

$$C_D = \frac{1}{\rho U_\infty{}^3} \int_0^\delta \frac{1}{T} \tau_{yx} \frac{du}{dy} dy \tag{3}$$

where the shear, τ_{yx}, consists of laminar and turbulent components and is given in terms of the fluid viscosity, μ, density, ρ, velocity gradient, du/dy and Reynolds shear stress, $\overline{u'v'}$ by,

$$\tau_{yx} = \mu \frac{du}{dy} - \rho \overline{u'v'} \tag{4}$$

This calculation of boundary layer dissipation is equally applicable for steady and unsteady flows if thermodynamic equilibrium is maintained and temporal gradients of internal energy can be neglected, as is the case here. With ensemble average measurements of mean velocities and Reynolds stress through the boundary layer, it is thus possible to calculate the ensemble average viscous boundary layer dissipation directly. In accordance with the derivation presented by Denton [11], the values of Reynolds stress used in the calculation are transformed to align with the local flow direction.

Figure 6 shows the dissipation coefficient, C_D, over the flat plate as calculated from the boundary layer measurements and equation (3). Also included on Figure 6 are the trajectory lines and labels from previous s-t diagrams. Immediately evident is the fact that high levels of viscous dissipation are predominantly confined to the wake induced turbulent wedge between line B and line D. The peak levels of C_D occur along line B because of the wake-induced transition. Another region of elevated C_D is associated with the large amplitude T-S waves observed at label F. These elevated levels of dissipation arise due to the mean flow transferring energy to the velocity oscillations (Betchov and Criminale [12]), however the levels of C_D associated with this energy transfer are about half of the peak levels measured. The calmed region between line D and line E has low levels of C_D. The magnitude is comparable to that of the undisturbed laminar boundary layer. Separated flows are typically associated with high levels of loss. However, the measurements presented in Figure 6 show that the regions of high shape factor in Figure 3, which are indicative of the initial stages of the formation of a separation bubble, have laminar levels of dissipation. These findings provide experimental proof of the loss reducing mechanism exploited in the design of high lift LP turbine blading. The highly dissipative separation bubble formed in the adverse pressure gradient of the steady flow is replaced between wake passing events initially by calmed flow and then the initial stages of the formation of a separation bubble, both of which are characterised by low levels of dissipation. Although the wake induced turbulent strip has high levels of dissipation, in the time average the losses are reduced by the longer durations of the calmed region and the initial stages of separation.

Further insight into the dissipation mechanism may be gained by looking at the measured profiles of velocity and Reynolds stress at selected points through a wake passing cycle at s/s_0=0.87. Five sets of profiles are plotted in Figure 7. The locations of these profiles are marked by numbered crosses on Figure 6. Profile 1 is associated with the calmed region and low levels of dissipation. The velocity profile is typical of the calmed region and has no

strong velocity gradients. The measured Reynolds stresses are low throughout the boundary layer at this location and so low levels of dissipation prevail.

The region of observed T-S waves at F has islands of moderate and low dissipation. Two profiles are considered from this region to show the source of the differences in Figure 7. Profile 2 is associated with higher levels of dissipation than profile 3, yet the velocity profiles are very similar and inflexional in character. The difference in dissipation results from the difference in the level of Reynolds stress. Profile 2 has a peak in Reynolds stress at the mid boundary layer height while 3 has lower levels more uniformly distributed over the inner half of the boundary layer height which has lower shear.

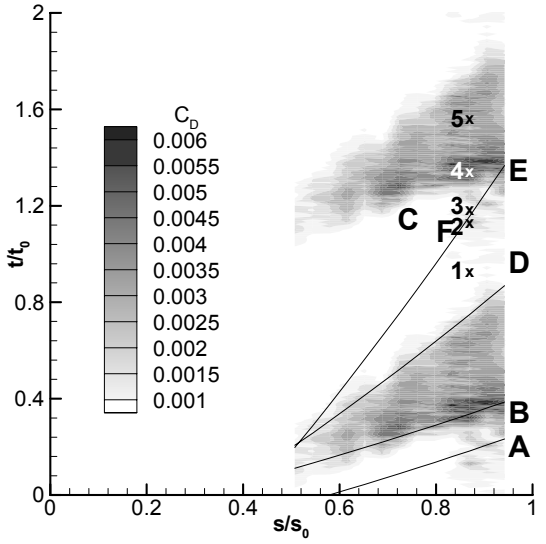

Figure 6: Space-time distribution of boundary layer dissipation coefficient.

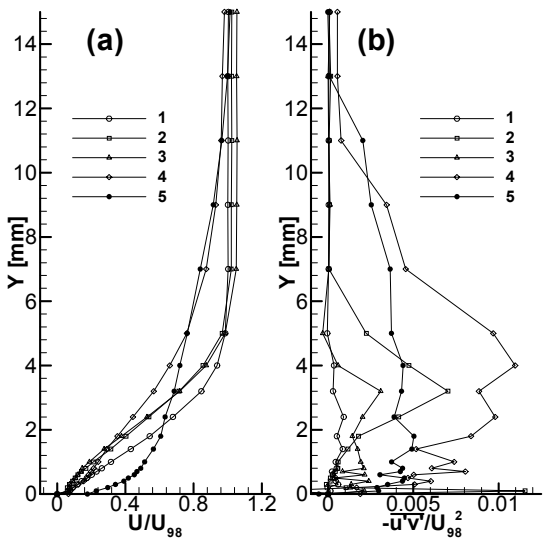

Figure 7: Profiles of (a) velocity and (b) Reynolds stress measured at s/s_0=0.87.

The peak levels of C_D are associated with profile 4 in Figure 7 and result from the laminar to turbulent transition. The boundary layer profile is not yet full like a typical turbulent profile, nor is it inflexional like profiles 2 and 3. The contribution from the profile shape is thus minor. The peak values of C_D are thus achieved primarily by the very high levels of Reynolds stress. However, due to the shape of the profile, the velocity gradients in the region of high Reynolds stress are also high, therefore, the peak levels of C_D are achieved through the combined effect of very high Reynolds stresses, and the relative location of the velocity gradients within the boundary layer.

The profile 5 in Figure 7 is taken from within the wake induced turbulent wedge. It is associated with a high level of C_D but with a noticeable non-turbulent contribution. The velocity profile at this location has a full, turbulent shape. The near wall velocity gradient is thus very high and this accounts for the non-turbulent contribution to C_D. The Reynolds stresses are high throughout the boundary layer height, although in the outer part of the boundary layer, the velocity gradients are low and thus the contribution to dissipation is diminished in this region.

Schlichting [15] gives a correlation for turbulent boundary layer dissipation with momentum thickness Reynolds number (Re_θ) in the range $10^3<Re_\theta<10^5$ and $1.2<H_{12}<2.0$ as

$$C_D = 0.0056\,\mathrm{Re}_\theta^{-1/6} \tag{5}$$

while for a laminar boundary layer Truckenbrodt [16] provides the correlation

$$C_D = \beta \mathrm{Re}_\theta^{-1} \tag{6}$$

where an analytic solution for a zero pressure gradient laminar boundary layer gives a coefficient β=0.173. Denton [11] suggests accounting for pressure gradients by considering the Pohlhausen velocity profiles so that $0.151 \leq \beta \leq 0.220$ for a highly decelerated to highly accelerated laminar boundary layers. These correlations are presented in Figure 8 together with the ensemble-averaged measurements of dissipation plotted against measured Re_θ. The dash-dot lines show the envelope for the laminar correlation as a function of pressure gradient. A circle indicates each measured data point and the scatter indicates the range of values measured. The points of highest Re_θ correspond to the wake-induced strip and have levels of C_D significantly higher than the correlation of Schlichting. The greatest density of measurement points lie in the range $200<\mathrm{Re}_\theta<300$ where the levels of C_D are laminar and in reasonable agreement with the correlation of Truckenbrodt.

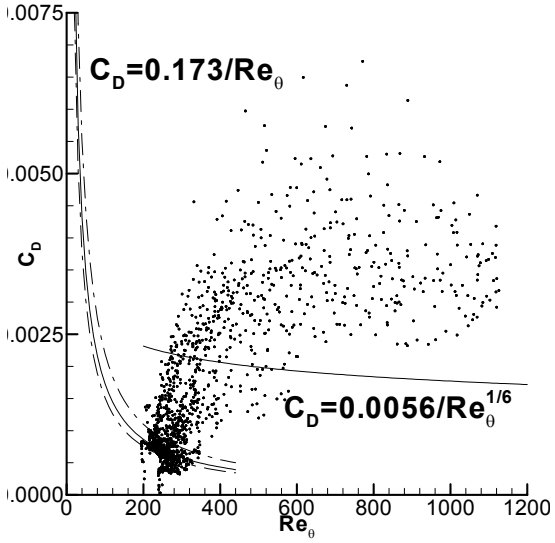

Figure 8: Measured C_D and correlations for laminar and turbulent boundary layers.

The measurements of C_D are thus in agreement with anticipated levels with the exception of those occurring during the wake-induced transition. These measurements are significantly higher than anticipated and the correlation of Schlichting, which is based on steady experimental data, is unable to capture the unsteady effects of wake-induced transition.

CONCLUSIONS

The interaction of a convected wake and LP turbine style boundary layer was found to be dominated by unsteady wake induced transition. Wake turbulence resulted in periodic bypass transition upstream of the separation point thus preventing the formation of a steady separation bubble.

A deterministic natural transition mechanism was identified in the boundary layer between wake passing events as it relaxed from turbulent to a laminar separating state. T-S wave packets were identified in the ensemble averaged velocity measurements. Their frequency was found to be in good agreement with that of the most amplified T-S wave in a Falkner-Skan profile of the same displacement thickness and the velocity fluctuations were

observed to grow exponentially thus indicating a linear stability mechanism is responsible for their formation and propagation.

Ensemble averaged measurements of velocity profiles and Reynolds stress profiles made along the surface of the flat plate using a rotated 1D LDA facilitated the calculation of the boundary layer dissipation coefficient. The space-time distribution of measured boundary layer dissipation provides experimental proof of the loss reducing mechanism associated with the calmed region and early stages of boundary layer separation.

REFERENCES

[1] Curtis, E.M., Hodson, H.P., Banieghbal, M.R., Denton, J.D. and Howell, R.J., 1996, *Development of blade profiles for low pressure turbine applications*, ASME paper 96-GT-358, International Gas Turbine and Aeroengine Congress and Exposition, Birmingham, UK

[2] Howell, R.J., Ramesh, O.N., Hodson, H.P., Harvey, N.W., Schulte, V., 2000, *High Lift and Aft Loaded Profiles for Low Pressure Turbines*, ASME 2000-GT-261

[3] Cobley, K., Coleman, N., Siden, G., Arndt, N., 1997, *Design of new three stage low pressure turbine for BMW Rolls-Royce BR715 engine*, ASME 97-GT-419

[4] Schulte, V. and Hodson, H.P., 1994, "Wake-Separation Bubble Interaction in Low Pressure Turbines", AIAA/SAE/ASME/ASEE 30th Joint Propulsion Conference and Exhibit, Indianapolis, Indiana

[5] Stieger, R.D. and Hodson, H.P. (2002), *Reynolds Stress Measurement with a Single Component Laser Doppler Anemometer.* The 16th Symposium on Measuring Techniques in Transonic and Supersonic Flow in Cascades and Turbines, 23-24 September 2002, Cambridge, England

[6] Gostelow, J.P., Melwani, N. and Walker, G.J., 1996, *Effects of streamwise pressure gradients on turbulent spot development*, ASME Journal of Turbomachinery, Vol. 118, pp. 737-743

[7] Hughes, J.D., Walker, G.J., 2000, *Natural transition phenomena on an axial compressor blade*, Presented at the International Gas Turbine and Aeroengine Congress and Exhibition, Munich, Germany, May 8-11, 2000-GT-264

[8] Walker, G.J., 1989, *Transitional flow in axial turbomachine blading*, AIAA Journal, vol. 27, no. 5, May

[9] Obremski, H.J., Morkovin, M.V. and Landhal, M., 1969, *A Portfolio of Stability Characteristics of Incompressible Boundary Layers*, AGARDograph 134, March

[10] Obremski, H.J., and Morkovin, M.V., 1969, *Application of quasi-steady stability model to periodic boundary layer flows*, AIAA Journal, Vol. 7, No. 7, pp 1298-1301, July

[11] Denton, J.D., 1993, *Loss mechanisms in turbomachines*, ASME Journal of Turbomachinery, Vol. 115, No. 4, pp 621-656

[12] Betchov, R. and Criminale, W.O., *Stability of Parallel Flows*, Academic Press, 1967

[13] Schulte, V., 1995, *Unsteady Separated Boundary Layers in Axial-flow Turbomachinery*, PhD Dissertation, Cambridge University

[14] Pauley, L.P., Moin, P. and Reynolds, W.C., 1990, *The structure of two-dimensional separation*, J. Fluid Mech. Vol. 220, pp. 397-411

[15] Schlichting, H., 1979, *Boundary-layer Theory*, McGraw-Hill, 7th Edition.

[16] Truckenbrodt, E., 1952, *A method of Quadrature for the calculation of laminar and turbulent boundary layers in Plane and Rotational Symmetric Flow*, Ingenieur-Archiv, Vol. 20, translated as NACA TM 1379